Development of a GWO-PID Optimization Controller for Suspension Stability Control of Electric Vehicle

1st Le Dinh Hieu
School of Engineering and Technology - Hue University
Hue city, Vietnam
ledinhhieu@hueuni.edu.vn

2nd Tran Quang Hung
School of Engineering and Technology - Hue University
Hue city, Vietnam
hungtran6152@gmail.com

***Abstract*—Automotive suspension systems can be classified into passive, semi-active, and active types, based on their ability to supply or dissipate energy during operation. Passive suspension systems typically employ passive components with fixed damping coefficients and spring stiffness, which limit passenger comfort and system stability. In contrast, active suspension systems can overcome these limitations, enabling smoother and safer vehicle operation. This study analyzes and compares the stability of passive and active suspension systems using a quarter-car model and proposes the design of a controller for the active suspension system under road excitation. The GWO-PID controller employs the Grey Wolf Optimizer (GWO) algorithm to optimally tune the parameters of the Proportional-Integral-Derivative (PID) controller. Simulation results in MATLAB/Simulink demonstrate that the GWO-PID controller improves the sprung mass acceleration by 21.06% compared with the PID controller and by 34.78% compared with the passive suspension system when traversing a 0.005 m speed bump in Scenario 1, as well as by 41.92% and 46.87% compared with the PID controller and passive suspension system, respectively, when traversing a 0.1 m speed bump in Scenario 2.**

Keywords—Electric vehicle suspension, Grey Wolf Optimizer, Optimized suspension, Modeling suspension.

I. INTRODUCTION

When traveling on the road, vehicles are often subjected to various external factors such as speed bumps, potholes, or road surface irregularities [1]. These impacts are transmitted to passengers through the suspension system, which functions to isolate the vehicle body from the wheels in order to minimize vibrations. An effective suspension system must simultaneously ensure the isolation of wheel vibrations from the vehicle body and minimize the influence of road disturbances, thereby enhancing ride comfort and handling performance [2]. Passenger comfort is maintained when the vertical forces transmitted from the road to the vehicle body are minimized, while the vertical displacement amplitude of the vehicle body and the suspension travel are controlled within optimal limits to preserve road holding and stability. Optimal tire–road contact at all four wheels must also be ensured.

Suspension systems are classified into three types: passive, semi-active, and active, depending on the level of external energy utilization [3]. Passive suspension systems employ springs and dampers with fixed parameters, requiring no power supply but facing limitations in simultaneously meeting ride comfort and stability demands across varying road conditions [4]. Semi-active suspension systems use adjustable dampers, allowing the damping characteristics to be altered according to operating conditions [5]. Active suspension systems incorporate actuators, typically hydraulic cylinders, arranged in parallel with the spring and damper to generate additional forces, thereby actively adjusting operating parameters [6]. With a closed-loop structure and a controller, active suspension systems can calculate and regulate the amount of energy to be dissipated or absorbed, overcoming the limitations of traditional suspension systems. Numerous studies have focused on improving suspension control performance for the quarter-car model by applying advanced control strategies [7]. Common methods include PID control, fuzzy control, sliding mode control, LQR, and optimization using intelligent algorithms [8].

This study designs, analyzes, and compares the characteristics of passive and active suspension systems on a quarter-car model, while proposing an optimal GWO-PID controller for the active suspension system under road excitation. Simulation results demonstrate that the active suspension system integrated with the GWO-PID controller achieves superior vibration suppression, improving sprung mass acceleration compared with the conventional PID controller and passive suspension system, while providing significant enhancements in ride comfort and vehicle stability.

II. DESIGN OF A QUARTER-CAR SUSPENSION SYSTEM

The quarter-car dynamic model is widely applied in studies of suspension vibration control [7]. As illustrated in Figure 1, the quarter-car configuration of a passive suspension system consists of two main masses: the sprung mass (ms) and the unsprung mass (mus). The suspension system is represented by a combination of a spring and a damper, while the tire is also modeled in a similar manner using an equivalent spring and damper.

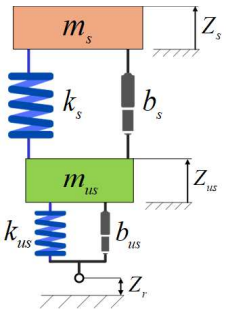

Fig. 1. Quarter-Car Passive Suspension Model.

In the case of a vehicle equipped with an active suspension system, an actuator is placed between the sprung mass and the unsprung mass, as shown in Figure 2. This

This paper is supported with research funding by Project code: B2024-DHH-11.

979-8-3315-6774-3/25/$31.00 ©2025 IEEE

actuator generates additional control forces to enhance ride comfort and driving stability.

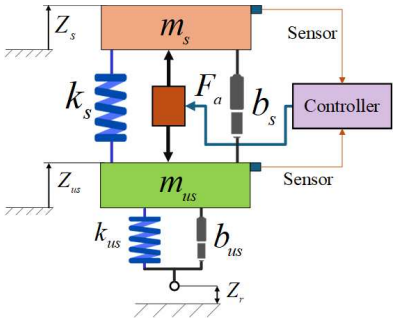

Fig. 2. Quarter-Car Active Suspension Model.

The dynamic characteristic equations of the quarter-car model are expressed as follows:

$$m_s\ddot{Z}_s = b_s\dot{Z}_{us} - b_s\dot{Z}_s - k_s\left(Z_s - Z_{us}\right) + F_a \tag{1}$$

$$\begin{aligned} m_{us}\ddot{Z}_{us} &= -b_s\dot{Z}_{us} - b_{us}\dot{Z}_s + b_s\dot{Z}_s + b_{us}\dot{Z}_r \\ &-k_s\left(Z_{us} - Z_s\right) - k_{us}\left(Z_{us} - Z_r\right) - F_a \end{aligned} \tag{2}$$

To analyze the model, the active suspension system is represented in state-space form based on the two equations of motion presented in (1) and (2).

A. Design of a PID Controller for an Active Suspension System

The PID controller is one of the most widely used control techniques in industry due to its simple structure, high reliability, ease of implementation, and low cost. In this study, the Ziegler–Nichols method is applied to calculate the parameters Kp, Ki, and Kd [9].

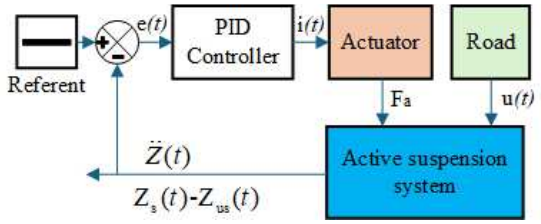

Fig. 3. Design of a PID Controller.

B. Design of a GWO-PID Controller for an Active Suspension System

The GWO algorithm is constructed based on the simulation of the social hierarchy and natural hunting strategy of gray wolves. This process can be generalized into three main stages: detecting, tracking, and approaching the prey (potential solutions); encircling and harassing the prey to weaken its resistance; and attacking and capturing the prey at the optimal moment [10]. During this process, the wolf pack maintains a hierarchical structure with three dominant individuals, alpha, beta, and delta, responsible for guiding the search strategy. The remaining wolves adjust their positions according to the three leaders, while the pack gradually converges toward the prey, with the final position of the alpha wolf considered the optimal solution.

Specifically, to expand the global search space, the wolf pack tends to disperse when |A| > 1. The encircling behavior of the prey is mathematically modeled by the following equations:

$$\begin{aligned} \vec{D} &= |\vec{C}\cdot\vec{X}_{pv}(T) - \vec{X}(T)| \\ \vec{X}(T+1) &= \vec{X}_{pv}(T) - \vec{A}\cdot\vec{D} \\ \vec{A} &= 2\vec{a}\cdot\vec{r}_1 - \vec{a} \\ \vec{C} &= 2\cdot\vec{r}_2 \end{aligned} \tag{3}$$

Where $\vec{A}$ and $\vec{C}$ are coefficient vectors, T denotes the current iteration number, $\vec{X}_{pv}$ represents the prey position vector, and $\vec{X}$ is the position vector of a wolf. To balance between exploration and exploitation, the parameter a is linearly decreased from 2 to 0 throughout the iterations. The position of each wolf in the population is updated relative to the prey position in the next iteration using the following mathematical expressions.

$$\begin{aligned} \vec{D}_\alpha &= |\vec{C}_1\cdot\vec{X}_\alpha - \vec{X}| \\ \vec{D}_\beta &= |\vec{C}_2\cdot\vec{X}_\beta - \vec{X}| \\ \vec{D}_\delta &= |\vec{C}_3\cdot\vec{X}_\delta - \vec{X}| \end{aligned} \tag{4}$$

$$\begin{aligned} \vec{X}_1 &= \vec{X}_\alpha - \vec{A}_1\cdot(\vec{D}_\alpha) \\ \vec{X}_2 &= \vec{X}_\beta - \vec{A}_2\cdot(\vec{D}_\beta) \\ \vec{X}_3 &= \vec{X}_\delta - \vec{A}_3\cdot(\vec{D}_\delta) \end{aligned} \tag{5}$$

$$\vec{X}(T+1) = \frac{\vec{X}_1 + \vec{X}_2 + \vec{X}_3}{3} \tag{6}$$

When |A| < 1, the wolf pack tends to narrow the search space and focus on exploiting the region around the prey. During this process, the agents in the GWO algorithm continuously update their positions under the guidance of the three elite individuals α, β, and δ, thereby executing the prey attack strategy to enhance convergence efficiency and the quality of the optimal solution. In this study, the GWO algorithm is implemented with a population size of 30 wolves and the number of iterations set to 100.

$$ITAE = \int_0^\infty t\,|e(t)|\,dt \tag{7}$$

The objective function selected for the system is the ITAE (Integral of Time-weighted Absolute Error) index, defined by the integral of the product between time and the absolute error as expressed in (7).

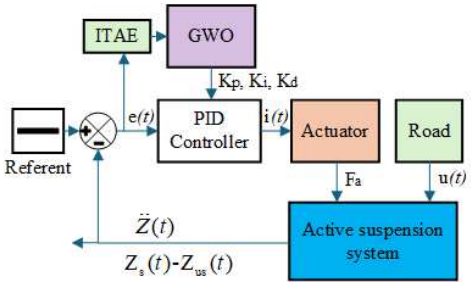

Fig. 4. Design of a GWO-PID controller.

III. SIMULATION RESULTS

This study proposes an improved optimal GWO-PID controller for the active suspension system and evaluates stability characteristics through state-space model simulations. The controller's effectiveness is directly compared with the conventional passive suspension system to highlight its advantages in vibration reduction and ride comfort enhancement. The evaluation is conducted under two independent test scenarios.

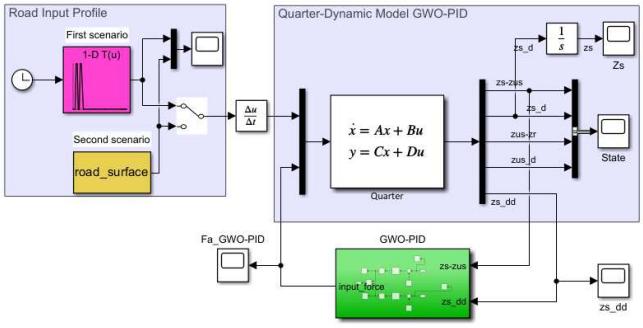

Fig. 5. Simulation diagram of the suspension system in MATLAB/Simulink.

TABLE I. THE CHARACTERISTIC PARAMETERS OF THE SUSPENSION SYSTEM ARE ESTABLISHED FOR THE SIMULATION PROCESS.

Parameters	Symbols	Unit	Values
Unsprung mass	m_{us}	kg	43
Sprung mass	m_s	kg	234
Suspension spring stiffness	k_s	kN/m	104
Suspension damping coefficient	b_s	kN/m	6.176
Tire stiffness	k_{us}	kN.s/m	400
Tire damping coefficient	b_{us}	N.s/m	0

In the first scenario, the excitation signal is selected as a clustered speed bump, commonly found at locations requiring vehicle speed reduction or serving as a warning before hazardous intersections, as well as in densely populated residential areas. In this simulation, the speed bump is assumed to have a fixed height of 0.005 m to ensure consistency in the analysis, as illustrated in Figure 6.

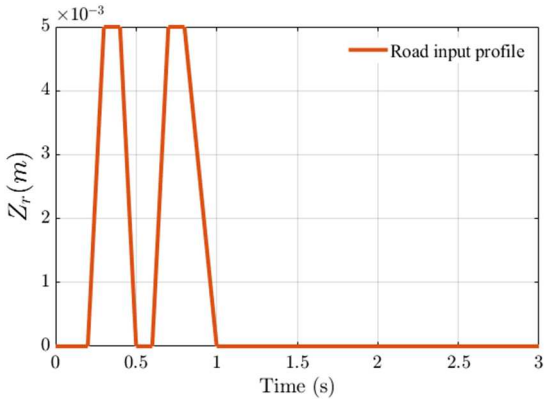

Fig. 6. Road surface displacement in the first scenario.

The comparison of sprung mass acceleration between the passive suspension system and the active suspension system is illustrated in Figure 7. The application of the GWO-PID algorithm to the active suspension system enhances ride comfort and passenger convenience when traversing a 0.005 m speed bump compared with the conventional PID algorithm and the passive suspension system. The overshoot of the GWO-PID algorithm is 0.8972 m/s², compared with −1.1366 m/s² for the PID controller and −1.3757 m/s² for the passive suspension system, representing improvements of 21.06% over the PID controller and 34.78% over the passive suspension system.

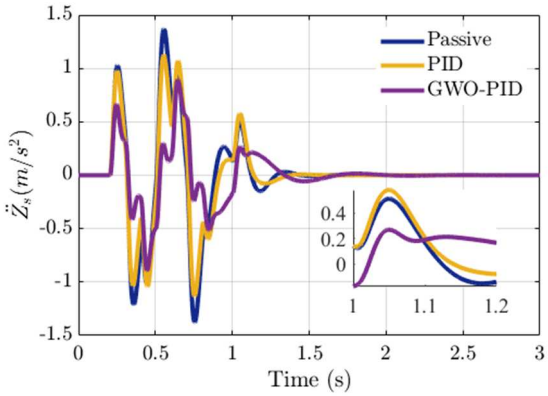

Fig. 7. Sprung mass acceleration in the first scenario.

Figure 8 presents the comparison of suspension travel between the passive and active systems. The results indicate that for the PID controller, the overshoot amplitude reaches −0.0022 m, while for the passive suspension system, it is −0.0017 m. In contrast, when applying the GWO-PID algorithm, the overshoot amplitude increases significantly to 0.0039 m, exceeding both the PID and passive cases. This demonstrates that although GWO-PID provides certain advantages in vibration control and improves passenger comfort, in terms of suspension travel, the algorithm generates a higher overshoot, which may affect the vehicle's dynamic stability.

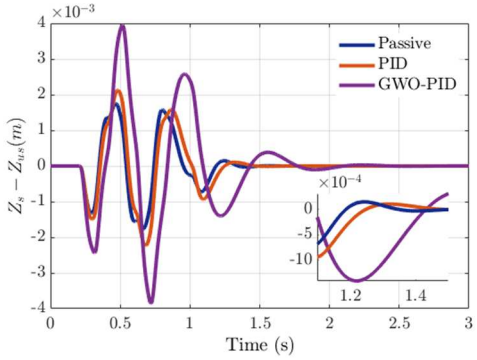

Fig. 8. Suspension travel in the first scenario.

TABLE II. OVERSHOOT AND STEADY-STATE ERROR DATA FOR SUSPENSION TRAVEL AND SPRUNG MASS ACCELERATION IN THE FIRST SCENARIO.

Suspension	Sprung mass acceleration		Suspension travel	
	Overshoot (m/s^2)	*Steady-state error (m)*	*Overshoot (m)*	*Steady-state error (m)*
Passive Suspension	-1.3757	2.1475e-09	-0.0017	-3.8145e-12
PID Active Suspension	-1.1366	1.0471e-09	-0.0022	-1.4896e-11
GWO-PID Active Suspension	0.8972	-4.9612e-05	0.0039	1.5881e-06

In the second scenario, the effect of the excitation signal is analyzed through the geometric profile model of the speed bump [11, 12]. This profile is constructed and represented in the form of a mathematical equation as follows (8):

$$z_r = \begin{cases} 0.05\times(1-\cos(7\pi t)) & If\ 1 \le t \le 1.09 \\ 0 & else \end{cases} \quad (8)$$

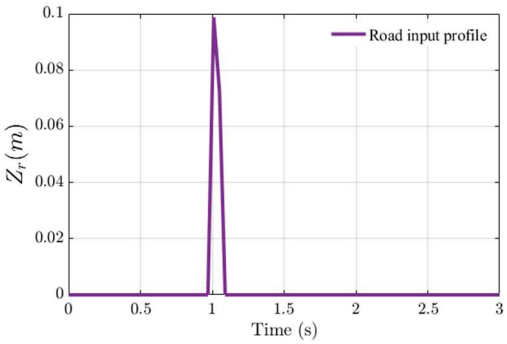

Fig. 9. Road surface displacement in the second scenario.

The comparison of sprung mass acceleration between the passive suspension system and the active suspension system is illustrated in Figure 10. The application of the GWO-PID algorithm to the active suspension system enhances ride comfort and passenger convenience when traversing the speed bump shown in Figure 9, compared with the conventional PID algorithm and the passive suspension system. The overshoot of the GWO-PID algorithm is 32.7414 m/s², compared with −56.3817 m/s² for the PID controller and −61.6301 m/s² for the passive suspension system, representing improvements of 41.92% over the PID controller and 46.87% over the passive suspension system.

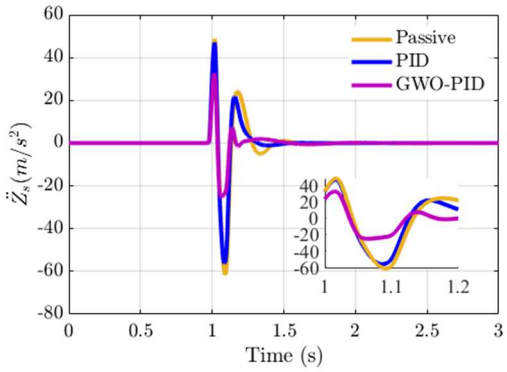

Fig. 10. Sprung mass acceleration in the second scenario.

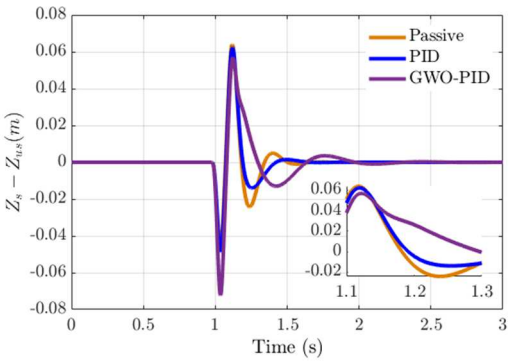

Fig. 11. Suspension travel in the second scenario.

The suspension travel in the second scenario between the passive suspension system and the active suspension system is illustrated in Figure 11. The GWO-PID controller exhibits an overshoot of −0.0720 m, which is greater than that of the conventional PID controller (0.0623 m) and the passive suspension system (0.0639 m). This indicates that although GWO-PID provides flexible control during the period from 1 s to 3 s, in this case, it produces a larger initial oscillation between 1 s and 1.09 s compared with the PID controller and the passive suspension system.

TABLE III. OVERSHOOT AND STEADY-STATE ERROR DATA FOR SUSPENSION TRAVEL AND SPRUNG MASS ACCELERATION IN THE SECOND SCENARIO.

Suspension	Sprung mass acceleration		Suspension travel	
	Overshoot (m/s^2)	*Steady-state error (m)*	*Overshoot (m)*	*Steady-state error (m)*
Passive Suspension	-61.6301	-3.0997e-07	0.0639	6.3814e-10
PID Active Suspension	-56.3817	1.5809e-07	0.0623	8.3889e-10
GWO-PID Active Suspension	32.7414	-0.0028	-0.0720	4.0201e-06

IV. CONCLUSION

In this study, a GWO-PID controller is developed for the active suspension system of an electric quarter-car model to be compared with the conventional PID controller and the passive suspension system. Simulations are conducted in MATLAB/Simulink under two input scenarios with different speed bumps to demonstrate the effectiveness of the proposed algorithm, using the overshoot of the sprung mass acceleration as an evaluation metric for passenger comfort. The GWO-PID controller improves the sprung mass acceleration by 21.06% compared with the PID controller and by 34.78% compared with the passive suspension system when traversing a 0.005 m speed bump in Scenario 1, and by 41.92% and 46.87% compared with the PID controller and passive suspension system, respectively, when traversing a 0.1 m speed bump in Scenario 2. These results demonstrate the superiority of the GWO-PID controller applied to the active suspension system, enhancing ride comfort and passenger convenience.

ACKNOWLEDGMENT

This paper is supported with research funding by Project code: B2024-DHH-11.

REFERENCES

[1] Y. Yin, W. Fu, X. Ma, J. Yu, X. Li, and Z. Dong, “Road Surface Pits and Speed Bumps Recognition Based on Acceleration Sensor,” IEEE Sensors Journal, vol. 24, no. 7, pp. 10669–10679, Feb. 2024, doi: https://doi.org/10.1109/jsen.2024.3362737.

[2] A. A. Ferhath and K. Kasi, “The evolution of damper technology for enhanced ride comfort and vehicle handling in vehicle suspension system,” International Journal of Dynamics and Control, vol. 12, no. 11, pp. 3908–3946, Aug. 2024, doi: https://doi.org/10.1007/s40435-024-01489-2.

[3] Z. Wang, C. Liu, X. Zheng, L. Zhao, and Y. Qiu, “Advancements in Semi-Active Automotive Suspension Systems with Magnetorheological Dampers: A Review,” Applied Sciences, vol. 14, no. 17, p. 7866, Sep. 2024, doi: https://doi.org/10.3390/app14177866.

[4] C. D. Kulkarni, P. P. Sail, A. V. Kalaskar, A. C. Mitra, and S. H. Gawande, “Real-time road testing and analysis of adjustable passive suspension system with variable spring stiffness,” JMST Advances,

vol. 6, no. 3, pp. 233–246, Aug. 2024, doi: https://doi.org/10.1007/s42791-024-00082-0.

[5] A. Soliman and M. Kaldas, “Semi-active suspension systems from research to mass-market – A review,” Journal of Low Frequency Noise, Vibration and Active Control, vol. 40, no. 2, pp. 1005–1023, Oct. 2019, doi: https://doi.org/10.1177/1461348419876392.

[6] D. N. Nguyen and T. A. Nguyen, “Evaluate the stability of the vehicle when using the active suspension system with a hydraulic actuator controlled by the OSMC algorithm,” Scientific Reports, vol. 12, no. 1, p. 19364, Nov. 2022, doi: https://doi.org/10.1038/s41598-022-24069-w.

[7] S. Jain, S. Saboo, C. I. Pruncu, and D. R. Unune, “Performance Investigation of Integrated Model of Quarter Car Semi-Active Seat Suspension with Human Model,” Applied Sciences, vol. 10, no. 9, p. 3185, May 2020, doi: https://doi.org/10.3390/app10093185.

[8] D. N. Nguyen and T. A. Nguyen, “The Dynamic Model and Control Algorithm for the Active Suspension System,” Mathematical Problems in Engineering, vol. 2023, p. e2889435, Feb. 2023, doi: https://doi.org/10.1155/2023/2889435.

[9] Hossein Nazemian and Masoud Masih-Tehrani, “Hybrid Fuzzy-PID Control Development for a Truck Air Suspension System,” SAE International journal of commercial vehicles, vol. 13, no. 1, May 2020, doi: https://doi.org/10.4271/02-13-01-0004.

[10] Sharif Naser Makhadmeh et al., “Recent advances in Grey Wolf Optimizer, its versions and applications: Review,” IEEE Access, pp. 1–1, Jan. 2023, doi: https://doi.org/10.1109/access.2023.3304889.

[11] M. A. Alim, M. A. Alim, and M. Abul Kawser, “Nonlinear Modeling and Analysis of Vehicle Vibrations Crossing Over a Speed Bump,” Journal of Vibration Engineering & Technologies, Sep. 2024, doi: https://doi.org/10.1007/s42417-024-01529-3.

[12] D. Wu, C. Liu, B. Qin, S. Zhong, X. Zhang, and Y. Du, “Fast calibration for vibration-based pavement roughness measurement based on model updating of vehicle dynamics,” International Journal of Pavement Engineering, vol. 25, no. 1, Dec. 2023, doi: https://doi.org/10.1080/10298436.2023.2287688.